Effects of Light-Emitting Diode Photobiomodulation Therapy and BioOss as Single and Combined Treatment in an Experimental Model of Bone Defect Healing in Rats

Uğur Havlucu, PhD[1]
Nilüfer Bölükbaşı, PhD[1]*
Sinem Yeniyol, PhD[1]
Şule Çetin, PhD[2]
Tayfun Özdemir, PhD[1]

The present study assesses histopathologically and histomorphometrically the effects of light-emitting diode (LED) photobiomodulation therapy (LPT) on bone healing in BioOss-filled femoral defects of rats. It has been reported that LPT modulates cellular metabolic processes, leading to an enhanced regenerative potential for biological tissues. Thirty-six male Wistar rats with femoral bone defects were divided into 4 groups: defect group (empty bone defect, without application of LPT), graft group (bone defect filled with BioOss, without application of LPT), (defect+LPT) group (empty bone defect, with application of LPT), and (graft+LPT) group (bone defect filled with BioOss, with application of LPT). An OsseoPulse LED device (wavelength: 618 nm; output power: 20 mW/cm^2) was initiated 24 hours postsurgery and performed every 24 hours for 7, 14, and 21 days. The LPT-applied and BioOss-filled defects presented a higher amount of new bone formation with trabeculae formation. These defects showed statistically significant lower values of inflammation severity, and fewer remnants of biomaterial were present. Within the limitations of this study, LPT has positive effects on bone healing histopathologically and histomorphometrically for the defects filled with BioOss 3 weeks after the rats' femora injury.

Key Words: light-emitting diode, photobiomodulation, deproteinized bovine bone graft, histomorphometry, histopathology

INTRODUCTION

Photobiomodulation has become a focus of scientific interest as a nonpharmacologic therapeutic method that can modulate fibroblast proliferation, attachment, and synthesis of collagen and procollagen; promote angiogenesis; and stimulate macrophages and lymphocytes by improving energy metabolism within the mitochondria at the cellular level. Well-accepted therapeutic tools for photobiomodulation are known as lasers and light-emitting diode (LED) arrays.[1]

The regulating mechanisms underlying the biostimulatory effects of photobiomodulation therapy are not clearly understood. It is reported that light in the near-infrared (NIR) range (630–1000 nm) is generated using lasers or LED arrays modulated cellular metabolic processes, and leads to an enhanced regenerative potential for biological tissues. Irradiation of red and NIR light is absorbed through cytochromes in the mitochondria, resulting in an increase of reactive oxygen species and adenosine triphosphate or cyclic adenosine monophosphate, and initiating signal transduction pathways that promote cellular proliferation and cytoprotection.[1–4]

Treatments based on photobiomodulation with lasers and LED arrays have shown similar responses. As suggested in the current literature, lasers and LED arrays have been extensively used to accelerate repair of soft tissues as well as to manage premalignant lesions of the oral cavity.[5–8] They have been used for their beneficial effects in clinical practice in orthodontics, distraction osteogenesis, methicillin-resistant *Staphylococcus aureus*–induced osteomyelitis, bisphosphonate-related osteonecrosis of the jaws, nonsurgical treatment of periodontitis, temporomandibular joint disorders, and after surgical extraction of lower third molars.[9–15] An effective alternative to lasers are LED arrays. They were originally developed by NASA for plant growth experiments in space.[16] Heat production from the laser light itself can actually damage tissue, and the pinpoint laser light beam can damage the eye.[17] Concerning these facts, recent studies started to apply LED arrays in orthodontics, bone grafting sites, angiogenesis, and wound healing as well as protection from apoptosis, retinal toxicity, and dioxin-induced developmental toxicity.[17–23]

Autogenous bone grafts are the material of choice as the gold standard in the treatment of bone defects, offering a source of osteogenic cells and osteoinductive substances without immunogenicity.[24,25] In 1965, Urist[26] reported that decalcified bone matrix implanted in nonbone sites induced

[1] Istanbul University, Faculty of Dentistry, Department of Oral Implantology, Istanbul, Turkey.
[2] Marmara University, School of Medicine, Department of Histology and Embryology, Istanbul, Turkey.
* *Corresponding author,* e-mail: dr.niluferbolukbasi@hotmail.com
DOI: 10.1563/AAID-JOI-D-13-00310

bone and cartilage formation, a process known as osteoinduction. In this respect, considerable interest has risen in the use of bone graft substitutes to fill critical bone defects because of their osteoinductive properties since autogeneous bone grafts had considerable limitations as donor sites.[27,28] Deproteinized bovine bone grafts have been widely used in the field of implantology and periodontology for the treatment of bone defects with predictable outcomes. BioOss, a porous bone mineral matrix of cortical or spongy bovine bone, is one of the most commonly used bovine bone graft materials, allowing rapid clot stabilization and revascularization and leading to osteoblast migration and osteogenesis in turn.[29]

On the other hand, LED photobiomodulation therapy (LPT) is a promising treatment that accelerates bone healing with desired quantity and quality. It may offer advantages as an attractive treatment option in previously grafted bone defect sites, allowing successful implant placement and osseointegration. Accordingly, in this present study, our aim was to study histopathologically and histomorphometrically the effects of LPT on the healing of bone defects treated with or without the deproteinized bovine bone graft BioOss in a rat model.

Materials and Methods

The research proposal was approved by the Ethics in Animal Research Committee of Istanbul University, Turkey (process No. 160/2010, November 4, 2010).

Experimental groups

The animals were distributed randomly into 4 experimental groups ($n_{animal} = 9$ and $n_{defect} = 36$, per group) named as follows:

- *Defect group:* Empty bone defect, without application of LPT
- *Graft group:* Bone defect filled with BioOss, without application of LPT
- *(Defect+LPT) group:* Empty bone defect, with application of LPT
- *(Graft+LPT) group:* Bone defect filled with BioOss, with application of LPT

The bone defects on the right femur served as untreated controls. The bone defects on the left femur were treated with LPT. LPT was initiated 24 hours after surgery and was performed for 7 sessions (1 week), 14 sessions (2 weeks), and 21 sessions (3 weeks), with an interval of 24 hours.

Surgery

This study was performed on 36 Wistar male rats (6–8 months, weighing 300–350 g). Surgery was performed under sterile conditions, and general anesthesia was induced by intramuscular injection of xilazin HCl (Alfazyne, 5 mg/kg, intramuscularly [IM]) and ketamin (Alfamine, at 40 mg/kg, IM). Cefazolin (16 mg/kg) was administered 30 minutes before the operation for infection prophylaxis. After shaving and asepsis with 70% alcohol solution, the distal sides of the right and left femora were exposed through a 15- to 10-mm longitudinal incision on the skin and muscle tissue. Two bone defects were prepared per each right and left femora of the rats. Standardized bone defects 3 mm in diameter and 3 mm in depth were produced vertically by using a round drill 3 mm in diameter at low speed (450 rpm/min) under continuous irrigation with sterile saline. One of the bone defects prepared at both femora was grafted with deproteinized bovine bone (BioOss, Geistlich Biomaterials, Wolhusen, Sweden), while the other defect was left empty (Figure 1). The periosteum and the skin were repositioned and sutured with 4-0 polyglycolic acid sutures (Medsorb PGLA, Medeks, Istanbul, Turkey). The animals were kept in separate cages at a temperature of 24°C ± 2°C with a light-dark period of 12 hours under standard diet and with free access to water throughout the study.

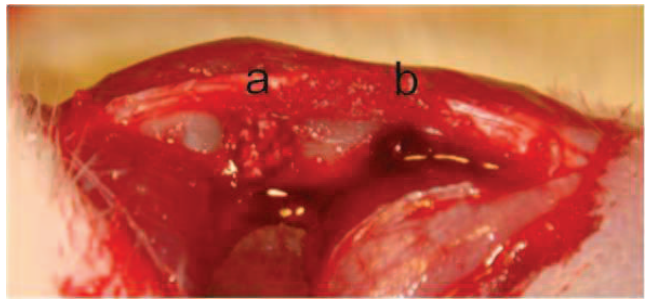

Figure 1. Standardized 3-mm diameter bone defects: (a) defect filled with BioOss; (b) empty defect.

Laser treatment

LPT was applied by placing the treatment array in contact with the site of the bone defect. Bone defects at the test site were treated with an OsseoPulse LED device (Biolux Research Ltd, Bone Regeneration System, Vancouver, Canada) with a wavelength of 618 nm (20 mW/cm^2 output power) applied at an irradiation period of 20 minutes. The resulting total dosage to the surface of the test site was 24 J/cm^2 per day with the treatment over a surface area of 3.6 cm^2. On days 8, 15, and 22 postsurgery, rats were killed with an intraperitoneal injection of sodium pentotalin (135 mg/kg). The femora were defleshed, and soft tissues were removed for analysis.

Histopathological analysis

Samples fixed in 10% buffer formalin for 4 weeks, and decalcification was performed by tissue decalcifier (Shandon TBD-1 Rapid Decalcifier, Thermo Scientific). The specimens were dehydrated in serial ethanol concentrations (70%, 90%, 96%, 100%) and embedded in paraffin blocks at room temperature.

Slices obtained in 5 μm were stained by hematoxylin and eosin, and the histopathological analysis was performed by semiquantitative methods by a histologist (blinded to the treatment of each group) under a light microscope (Olympus BX51, Optical Co Ltd, Tokyo, Japan). Remnants of biomaterials, new bone formation, and the severity of the inflammation were scored for each animal. The scores for new bone formation were determined by counting the associated cells and their ratio to the total cell count in a standardized area at various magnifications. Remnants of biomaterials, new bone formation, and severity of the inflammation have been given − (0%), + (1%–30%), ++ (30%–60%), or +++ (>60%) scores according to their surface covering, as previously described by Cankaya et al.[30]

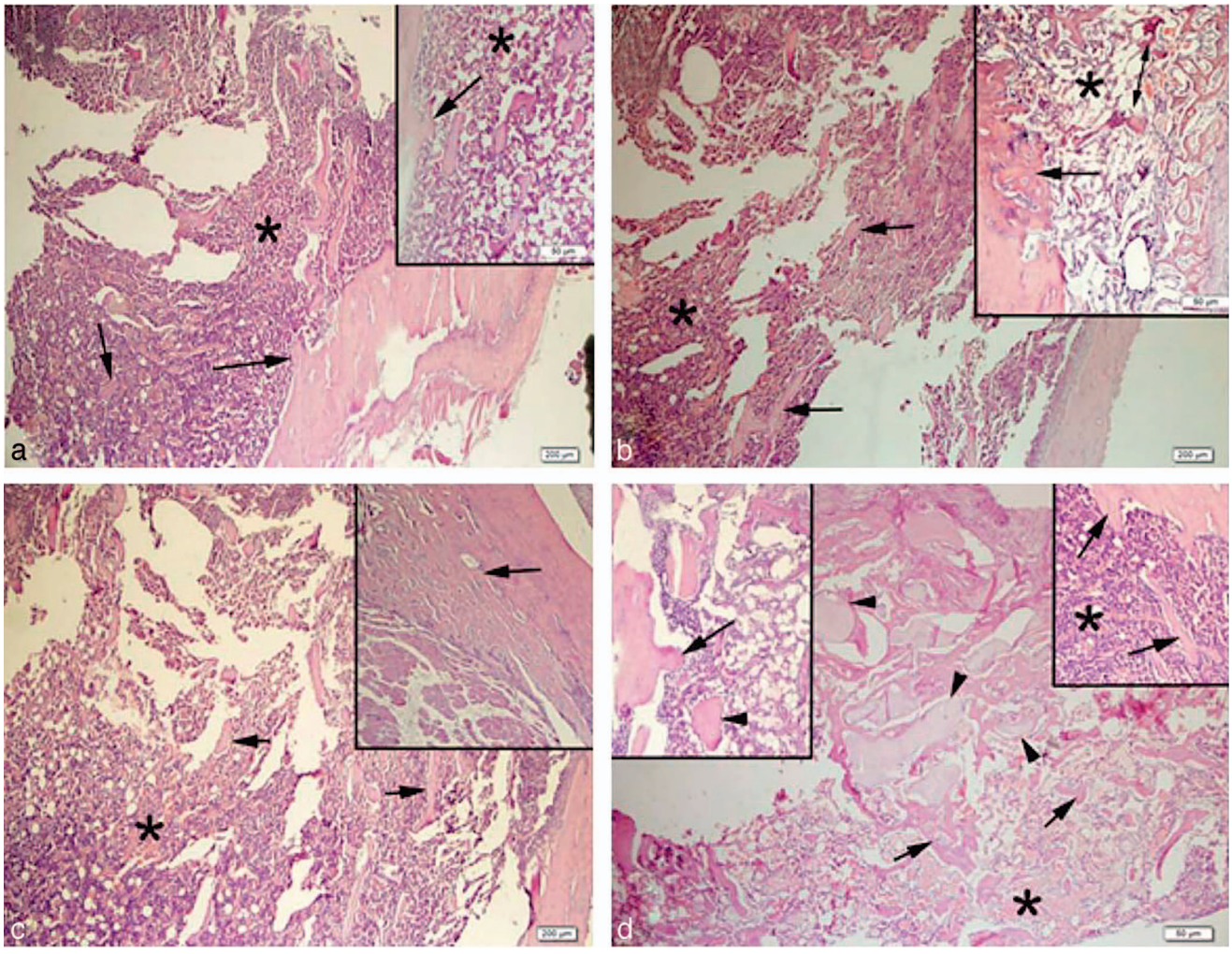

Figure 2. (a) Photomicrographs of bone tissue sections from femurs of animals in week 1 stained with hematoxylin and eosin in the defect group, showing details of severe inflammatory infiltrate areas (asterisks) and minimal vascularization (asterisks) as well as new bone with weak trabecular structure (arrows; magnifications; ×40 and ×200). (b) Photomicrographs of bone tissue sections from femurs of animals in week 1 stained with hematoxylin and eosin in the graft group, showing details of severe inflammatory infiltrate areas (asterisks), moderate vascularization (asterisks), and pronounced new bone formation and trabecular bone structure (arrows) as well as remnants of biomaterial in some areas (double arrow; magnifications: ×40 and ×200). (c) Photomicrographs of bone tissue sections from femurs of animals in week 1 stained with hematoxylin and eosin in the (defect+light-emitting diode photobiomodulation therapy [LPT]) group, showing details of severe inflammatory infiltrate areas (asterisks) and moderate vascularization (asterisks) as well as an increase in osteoblasts and trabecular bone structure (arrows; magnifications: ×200 and ×400). (d) Photomicrographs of bone tissue sections from femurs of animals in week 1 stained with hematoxylin and eosin in the (graft+LPT) group, showing details of severe inflammatory infiltrate areas (asterisks), moderate vascularization (asterisks), pronounced trabecular bone structure, and presence of osteoblasts (arrows) as well as remnants of biomaterial in some areas (arrow heads; magnifications: ×200 and ×400).

Statistical analysis

Statistical analysis was performed by SPSS 15.0 (SSPS Inc, Chicago, Ill) for Windows. The differences between the groups were analyzed by χ^2 test followed by Fisher exact χ^2 test. Statistical significance was considered at a probability $P < .05$.

Results

General findings

In all 36 rats, no postoperative complications were observed, yielding a total of 144 bone defects for final analysis. Wound healing progressed without any sign of infection. No weight loss and no side effects, such as behavioral changes, or features of pain were observed.

Histopathological analysis

One Week After Creating the Defects

Figure 2a–d shows the characteristic histologic sections for all the groups at the end of 1 week. Histologic and morphometric analysis of the defect group showed the presence of loose connective tissue with rich neovascularization and areas of newly formed bone tissue comprising thin trabecular structure, with the presence of severe inflammatory reaction.

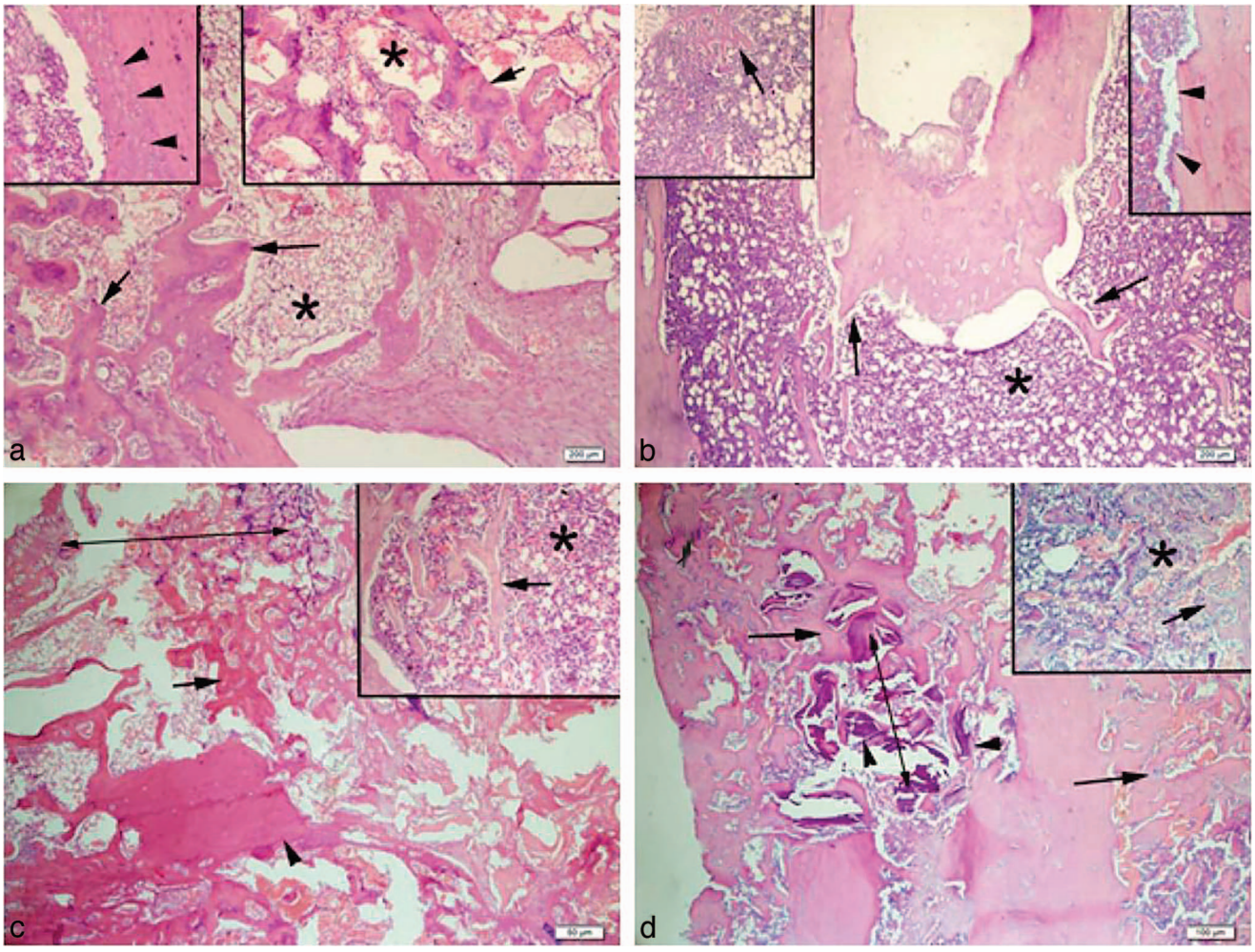

Figure 3. (a) Photomicrographs of bone tissue sections from femurs of animals in week 2 stained with hematoxylin and eosin in the defect group, showing details of severe inflammatory infiltrate areas (asterisks), moderate vascularization (asterisks), and osteoblastic activity (arrows), as well as new osteocyte (arrow heads) formations (magnifications: ×40 and ×200). (b) Photomicrographs of bone tissue sections from femurs of animals in week 2 stained with hematoxylin and eosin in the graft group, showing details of severe inflammatory infiltrate areas (asterisks), moderate vascularization (asterisks), as well as presence increased osteoblastic activity (arrow heads) and osteoid matrix formation (arrows; magnifications: ×200 and ×400). (c) Photomicrographs of bone tissue sections from femurs of animals in week 2 stained with hematoxylin and eosin in the (defect+light-emitting diode photobiomodulation therapy [LPT]) group, showing details of severe inflammatory infiltrate areas (asterisks), moderate vascularization (asterisks), well-developed trabecular bone structure (arrow head), and osteoblastic activity (arrows) as well as remnants of biomaterials (double arrow; magnifications: ×40 and ×200). (d) Photomicrographs of bone tissue sections from femurs of animals in week 2 stained with hematoxylin and eosin in the (graft+LPT) group, showing details of severe inflammatory infiltrate areas (asterisks), severe vascularization (asterisks), pronounced trabecular bone structure (arrows), as well as remnants of biomaterial in some areas (double arrow; magnifications: ×100 and ×200).

The graft group presented a defect site filled with granulation tissue and remnants of biomaterial. In a few areas, circumferential new bone formations, separated by appositional lines, were observed around the biomaterials.

The (defect+LPT) group showed the presence of loose connective tissue with rich neovascularization as well as lymphocyte and plasma cell infiltration. Trabecular bone formation was more abundantly observed at the defect walls. Bone marrow rich in cells was detected at the medullar space.

The (graft+LPT) group showed the presence of loose connective tissue with rich neovascularization and inflammatory cells, presenting remnants of biomaterial. Circumferential new bone formation was observed in contact with the biomaterials.

Two Weeks After Creating the Defects

Figure 3a through d shows the characteristic histologic sections for all the groups at the end of 2 weeks. The (defect+LPT) group showed results similar to the defect group. New bone formation in the (defect+LPT) group was more evident than in the defect group.

New bone formation in the (graft+LPT) group was found to be greater than in the graft group. Remnants of biomaterial were observed in both the graft group and the (graft+LPT) group. In both groups, the presence of severe inflammatory infiltrate was detected.

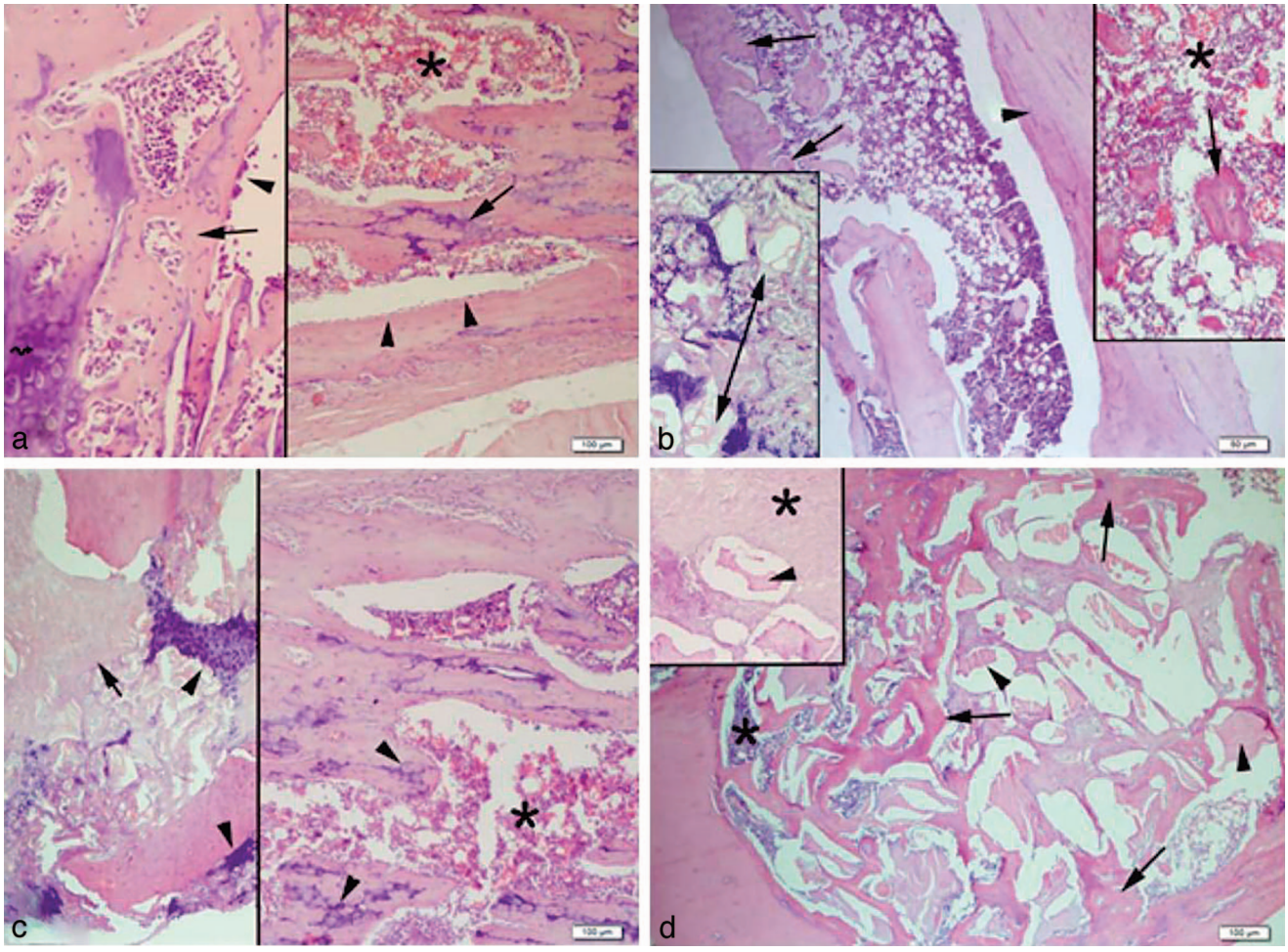

Figure 4. (a) Photomicrographs of bone tissue sections from femurs of animals in week 3 stained with hematoxylin and eosin in the defect group, showing details of severe inflammatory infiltrate areas (asterisks) and moderate vascularization (asterisks) as well as well-organized trabecular bone structure (arrows), osteoblasts (arrow heads), and osteocytes embedded inside the osteoid matrix (wavy line; magnifications: ×100 and ×200). (b) Photomicrographs of bone tissue sections from femurs of animals in week 3 stained with hematoxylin and eosin in the graft group, showing details of severe inflammatory infiltrate areas (asterisks), moderate vascularization (asterisks), well-developed trabecular bone structure (arrows), and osteoid matrix formation (arrow head) as well as remnants of biomaterial in some areas (double arrow; magnifications: ×100 and ×200). (c) Photomicrographs of bone tissue sections from femurs of animals in week 3 stained with hematoxylin and eosin in the (defect+light-emitting diode photobiomodulation therapy [LPT]) group, showing details of severe inflammatory infiltrate areas (asterisks) and moderate vascularization (asterisks) as well as well-developed trabecular bone structure (arrows) and osteoblastic activity (arrow heads; magnifications: ×200 and ×400). (d) Photomicrographs of bone tissue sections from femurs of animals in week 3 stained with hematoxylin and eosin in the (graft+LPT) group, showing details of severe inflammatory infiltrate areas (asterisks) and severe vascularization (asterisks), pronounced trabecular bone structure, and presence of osteoid matrix formation (arrows) as well as remnants of biomaterial (arrow heads) inside the trabecular bone (magnifications: ×100 and ×200).

Three Weeks After Creating the Defects

Figure 4a through d shows the characteristic histologic sections for all the groups at the end of 3 weeks. Empty defects in both the defect group and (defect+LPT) group were filled with new bone trabeculae. Osteoclasts were observed at some areas around the newly formed bone tissue. Inflammatory cells were observed inside the area of inflammatory infiltrate.

The graft group and (graft+LPT) group showed remnants of biomaterial surrounded by bone trabeculae on the periphery aligned by active osteoblasts. Defect sites were mostly reconstituted with new bone tissue, and osteoclasts were observed.

Histomorphometric analysis

There were statistical differences between the groups for all of the time intervals (Table 1). The defect group showed significantly less new bone formation than that of the graft group and (graft+LPT) group at all time points (first week, $P < .05$ and $P < .01$, respectively, second week and third week, $P < .01$, all). The (defect+LPT) group showed significantly less new bone formation than the graft group and (graft+LPT) group for the second week ($P < .05$, all) and that of the (graft+LPT) group at the third week ($P < .01$).

There were statistical differences between the groups for the second and third weeks for the severity of inflammation

Table 1

Histopathological findings of the groups for the new bone formation for the 3 time intervals: − (0%), + (1%–30%), ++ (30%–60%), +++ (>60%)

Week	Defect Group n (%)	Graft Group n (%)	(Defect+LPT) Group n (%)	(Graft+LPT) Group n (%)	
1					
(−)	3 (25.00)	0 (0.00)	2 (16.70)	0 (0.00)	χ^2: 21,067 $P = .012$*
(+)	9 (75.00)	8 (66.70)	7 (58.30)	4 (33.30)	
(++)	0 (0.00)	4 (33.30)	3 (25.00)	5 (41.70)	
(+++)	0 (0.00)	0 (0.00)	0 (0.00)	3 (25.00)	
2					
(+)	7 (58.30)	0 (0.00)	5 (41.70)	0 (0.00)	χ^2: 27,917 $P = .001$**
(++)	5 (41.70)	12 (100.00)	7 (58.30)	8 (66.70)	
(+++)	0 (0.00)	0 (0.00)	0 (0.00)	4 (33.30)	
3					
(+)	3 (25.00)	0 (0.00)	0 (0.00)	0 (0.00)	χ^2: 27,158 $P = .001$**
(++)	8 (66.70)	4 (33.30)	7 (58.30)	0 (0.00)	
(+++)	1 (8.30)	8 (66.70)	5 (41.70)	12 (100.00)	

*$P < .05$; **$P < .01$.

(Table 2). The (graft+LPT) group showed significantly less severity of inflammation than the defect group and graft group for the second week ($P < .05$, all), whereas it was significantly less than the defect group and (defect+LPT) group at the third week ($P < .01$, all).

Remnants of biomaterials were found to be significantly greater for the graft group compared with that of the (graft+LPT) group for the third week ($P < .05$; Table 3).

Discussion

The use of photobiomodulation therapy, applied by LPT and low-level laser therapy (LLLT), has been suggested as a way of accelerating and improving the bone tissue-healing process to reduce the healing time. The present study was conducted to study the influence of LPT on bone healing in rat femoral bone defects filled with BioOss histopathologically and histomorphometrically.

Low-level laser therapy has recently emerged as a therapeutic approach in oral implantology. It has been reported to abbreviate the bone repair process by stimulating the modulation of the initial inflammatory response.[31] Positive effects on callus development and enhanced stiffness of repairing tissue have been observed.[32,33] A larger attachment with the peri-implant bone tissue has been shown at the low-level laser–treated implant sites.[34] Similarly, higher osteocyte viability has been observed in the irradiated peri-implant bone, reducing the healing time.[35] Immunohistochemical studies have confirmed LLLT's potential to increase the expression of receptor activator of nuclear factor-kB ligand (RANK), the receptor activator of nuclear factor kB ligand (RANKL), and osteoprotegerin (OPG) as well as formation of higher bone density after installation of dental titanium implants.[36]

Low-level laser therapy in combination with bone grafting has been applied at inadequate bony sites in order to regenerate the bone for dental implant placements. Low-level laser therapy on bone defects grafted with PerioGlas has been reported to significantly accelerate bone healing.[37] According to Márquez Martínez et al,[38] increased amounts of collagen fibers, bone trabeculae formation, and osteoblastic activity have been detected with infrared laser photobiomodulation in bone defects filled with Genox. Application of LLLT in combination with Bio-Oss has been reported to increase expressions of the RANKL,

Table 2

Histopathological findings of the groups for the severity of inflammation for the 3 time intervals: − (0%), + (1%–30%), ++ (30%–60%), +++ (>60%)

Week	Defect Group n (%)	Graft Group n (%)	(Defect+LPT) Group n (%)	(Graft+LPT) Group n (%)	*P*
1					
(−)	3 (25.00)	0 (0.00)	0 (0.00)	0 (0.00)	χ^2: 8,048 $P = .056$
(+)	0 (0.00)	0 (0.00)	2 (16.70)	0 (0.00)	
(++)	2 (16.70)	3 (25.00)	1 (8.30)	3 (25.00)	
(+++)	7 (58.30)	9 (75.00)	9 (75.00)	9 (75.00)	
2					
(++)	6 (50.00)	7 (58.30)	8 (66.70)	12 (100.00)	χ^2: 21,575 $P = .045$*
(+++)	6 (50.00)	5 (41.70)	4 (33.30)	0 (0.00)	
3					
(+)	0 (0.00)	8 (66.70)	5 (41.70)	12 (100.00)	χ^2: 25,628 $P = .001$**
(++)	12 (100.00)	4 (33.30)	7 (58.30)	0 (0.00)	

*$P < .05$; **$P < .01$.

TABLE 3

Histopathological findings of the groups for the remnants of biomaterials for the 3 time intervals: − (0%), + (1%–30%), ++ (30%–60%), +++ (>60%)

Week	Graft Group n (%)	(Graft+LPT) Group n (%)	P
1			
(++)	4 (33.30)	6 (50.00)	χ^2: 0,686, $P = .408$
(+++)	8 (66.70)	6 (50.00)	
2			
(++)	9 (75.00)	12 (100.00)	Fishers exact $P = .217$
(+++)	3 (25.00)	0 (0.00)	
3			
(+)	7 (58.30)	12 (100.00)	Fisher exact $P = .037$*
(++)	5 (41.70)	0 (0.00)	

*$P < .05$.

OPG, and RANK as well as the density of bone, with a significantly higher mineralization index.[29,39,40]

Although lasers and LED arrays have similar biological responses, there are basic differences between them. Lasers emit coherent light, whereas the emission of LED arrays is not coherent.[41] Lasers are limited in their ability to reproduce combined wavelengths, and their beam width makes it difficult to treat large areas. As an effective alternative to lasers, LED arrays can produce light in the far-red to NIR at optimal wavelengths and energy densities. LED arrays can be constructed in various sizes to irradiate large areas, and they do not emit any heat, eliminating the danger of tissue damage, unlike lasers. LED arrays are more advantageous because of lower cost of equipment and energy consumption, and they have been approved for use in humans by the Food and Drug Administration.[1,8]

In this study, we used an OsseoPulse LED device (wavelength: 618 nm, output power: 20 mW/cm^2, t: 20 minutes), and the resulting total dosage applied to the surface of the test site was 24 J/cm^2 per day. The results demonstrated the stimulatory effects of LED photobiomodulation therapy on bone defects filled with BioOss. The authors assumed that BioOss acted as an osteoconductive framework for the deposition of new bone. However, the use of LPT positively affected the new bone formation with a highly vascularized connective tissue formation accompanied by lower severity of inflammation and lower amount of biomaterial remnants. This anti-inflammatory effect at the earlier periods of the bone-healing process and rapid resorption of the biomaterial could be attributed to the light-enhanced ATP, DNA, and RNA synthesis, due to the increased mitochondrial activities and the changes in cytoplasm through the absorption of the light by the photoreceptors, as previously described by Karu.[42]

In the literature, results regarding the use of photobiomodulation therapy with LED arrays have been published. Since we were unable to find many previous reports in the literature concerning the use of LED arrays associated with bone-grafting procedures, it makes our discussion of the results very difficult in this regard. In one such study, LED light alone or in association with mineral trioxide aggregate was found to cause less inflammation, increased collagen deposition, and improved deposition of calcium hydroxyapatite in the healing bone.[19,43] OsseoPulse LED device photobiomodulation was found to enhance bone formation and particle resorption in hydroxyapatite particulate–grafted fresh extraction sockets.[44] In another study of the OsseoPulse LED device, a favorable effect on healing and stability of titanium orthodontic miniscrews was reported.[45] The results of our study and those of others indicated that bone irradiated with LED arrays showed increased neovascularization, collagen deposition, and bone neoformation compared with nonirradiated bone. In addition to these studies, our results have demonstrated that the use of BioOss is effective in the healing of bone defects and that combining it with LPT improves the outcomes of this therapeutic approach.

Photobiomodulation is dependent on physical parameters (ie, wavelength, output power, and energy density), and it is crucial to know the correct combination of parameters.[46] Similar to the lasers, the interpretation of differences between reported studies for LED arrays may be related to the difference in these parameters, graft types, and animal models used, creating difficulties in hindering the comparison of treatment outcomes and extrapolation to the clinical practice in humans.[47] The question here shall be identifying the optimal light and experimental parameters for the optimal biological outcomes.

Conclusions

This investigation used an LPT, suggesting that a wavelength of 618 nm is effective in enhancing bone healing in BioOss-filled bone defects in rat femora, as depicted by histopathological and histomorphometric analysis, offering a substantial decrease in time required to place an implant.

As a major limitation of this study, additional data from in vivo human trials are required to validate this assumption. In addition, long-term viability and mechanical properties of the LPT-treated and BioOss-grafted bone defect sites should be further evaluated to contribute to a better understanding of the long-term clinical performance of these sites.

Abbreviations

IM: intramuscular
LED: light-emitting diode
LLLT: low-level laser therapy
LPT: light-emitting diode photobiomodulation therapy
NIR: near-infrared
OPG: osteoprotegerin
RANK: the expression of receptor activator of nuclear factor kB ligand
RANKL: the receptor activator of nuclear factor kB ligand

References

1. Desmet KD, Paz DA, Corry JJ, et al. Clinical and experimental applications of NIR-LED photobiomodulation. *Photomed Laser Surg*. 2006;24:121–128.

2. Karu TI. Mitochondrial signaling in mammalian cells activated by red and near-IR radiation. *Photochem Photobiol*. 2008;84:1091–1099.

3. Lavi R, Shainberg A, Friedmann H, et al. Low-energy visible light induces reactive oxygen species generation and stimulates an increase of intracellular calcium concentration in cardiac cells. *J Biol Chem*. 2003;278:40917–40922.

4. Gavish L, Asher Y, Becker Y, Kleinman Y. Low-level laser irradiation stimulates mitochondrial membrane potential and disperses subnuclear promyelocytic leukemia protein. *Lasers Surg Med*. 2004;35:369–376.

5. de Souza TO, Martins MA, Bussadori SK, et al. Clinical evaluation of low-level laser treatment for recurring aphthous stomatitis. *Photomed Laser Surg*. 2010;28:S85–S88.

6. Gouvêa de Lima A, Villar RC Jr, de Castro G, et al. Oral mucositis prevention by low-level laser therapy in head-and-neck cancer patients undergoing concurrent chemoradiotherapy: a phase III randomized study. *Int J Radiat Oncol Biol Phys*. 2012;82:270–275.

7. Cafaro A, Albanese G, Arduino PG, et al. Effect of low-level laser irradiation on unresponsive oral lichen planus: early preliminary results in 13 patients. *Photomed Laser Surg*. 2010;28:S99–S103.

8. Freire MD, Freitas R, Colombo F, Valença A, Marques AM, Sarmento VA. LED and laser photobiomodulation in the prevention and treatment of oral mucositis: experimental study in hamsters. *Clin Oral Investig*. 2014;18: 1005–1013.

9. Sousa MV, Scanavini MA, Sannomiya EK, Velasco LG, Angelieri F. Influence of low-level laser on the speed of orthodontic movement. *Photomed Laser Surg*. 2011;29:191–196.

10. Kreisner PE, Blaya DS, Gaião L, et al. Histological evaluation of the effect of low-level laser on distraction osteogenesis in rabbit mandibles. *Med Oral Patol Oral Cir Bucal*. 2010;15:616–618.

11. Kaya GŞ, Kaya M, Gürsan N, Kireççi E, Güngörmüş M, Balta H. The use of 808-nm light therapy to treat experimental chronic osteomyelitis induced in rats by methicillin-resistant *Staphylococcus aureus*. *Photomed Laser Surg*. 2011;29:405–412.

12. Vescovi P, Manfredi M, Merigo E, et al. Early surgical laser-assisted management of bisphosphonate-related osteonecrosis of the jaws (BRONJ): a retrospective analysis of 101 treated sites with long-term follow-up. *Photomed Laser Surg*. 2011;30:5–13.

13. Makhlouf M, Dahaba MM, Tunér J, Eissa SA, Harhash TA. Effect of adjunctive low level laser therapy (LLLT) on nonsurgical treatment of chronic periodontitis. *Photomed Laser Surg*. 2012;30:160–166.

14. Brignardello-Petersen R, Carrasco-Labra A, Araya I, Yanine N, Beyene J, Shah PS. Is adjuvant laser therapy effective for preventing pain, swelling, and trismus after surgical removal of impacted mandibular third molars? A systematic review and meta-analysis. *J Oral Maxillofac Surg*. 2012; 70:1789–1801.

15. Salmos-Brito JA, de Menezes RF, Teixeira CE, et al. Evaluation of low-level laser therapy in patients with acute and chronic temporomandibular disorders. *Lasers Med Sci*. 2013;28:57–64.

16. Wong-Riley MT, Liang HL, Eells JT, et al. Photobiomodulation directly benefits primary neurons functionally inactivated by toxins: role of cytochrome c oxidase. *J Biol Chem*. 2005;280:4761–4771.

17. Eells JT, Wong-Riley MT, VerHoeve J, et al. Mitochondrial signal transduction in accelerated wound and retinal healing by near-infrared light therapy. *Mitochondrion*. 2004;4:559–567.

18. Ekizer A, Uysal T, Güray E, Akkuş D. Effect of LED-mediated-photobiomodulation therapy on orthodontic tooth movement and root resorption in rats. *Lasers Med Sci*. 2015;30:779–785.

19. Pinheiro AL, Soares LG, Barbosa AF, Ramalho LM, dos Santos JN. Does LED phototherapy influence the repair of bone defects grafted with MTA, bone morphogenetic proteins, and guided bone regeneration? A description of the repair process on rodents. *Lasers Med Sci*. 2012;27:1013–1024.

20. Corazza AV, Jorge J, Kurachi C, Bagnato VS. Photobiomodulation on the angiogenesis of skin wounds in rats using different light sources. *Photomed Laser Surg*. 2007;25:102–106.

21. Liang HL, Whelan HT, Eells JT, et al. Photobiomodulation partially rescues visual cortical neurons from cyanide-induced apoptosis. *Neuroscience*. 2006;139:639–649.

22. Eells JT, Henry MM, Summerfelt P, et al. Therapeutic photobiomodulation for methanol-induced retinal toxicity. *Proc Natl Acad Sci U S A*. 2003;100:3439–3444.

23. Yeager RL, Franzosa JA, Millsap DS, et al. Survivorship and mortality implications of developmental 670-nm phototherapy: dioxin co-exposure. *Photomed Laser Surg*. 2006;24:29–32.

24. Iwama T, Yamada J, Imai S, Shinoda J, Funakoshi T, Sakai N. The use of frozen autogenous bone flaps in delayed cranioplasty revised. *Neurosurgery*. 2003;52:591–596.

25. Mercer C. Lasers in dentistry: a review part 1. *Dent Update*. 1996;23: 74–80.

26. Urist MR. Bone: formation by autoinduction. *Science*. 1965;12:893–899.

27. Johansson B, Grepe A, Wannfors K, Hirsch JM. A clinical study of changes in the volume of bone grafts in the atrophic maxilla. *Dentomaxillofac Radiol*. 2001;30:157–161.

28. Raghoebar GM, Meijndert L, Kalk WW, Vissink A. Morbidity of mandibular bone harvesting: a comparative study. *Int J Oral Maxillofac Implants*. 2007;22:359–365.

29. Rasouli Ghahroudi AA, Rokn AR, Kalhori KA, et al. Effect of low-level laser therapy irradiation and Bio-Oss graft material on the osteogenesis process in rabbit calvarium defects: a double blind experimental study. *Lasers Med Sci*. 2014;29:925–932.

30. Cankaya AB, Erdem MA, Isler SC, et al. Use of cone-beam computerized tomography for evaluation of bisphosphonate-associated osteonecrosis of the jaws in an experimental rat model. *Int J Med Sci*. 2011;8: 667–672.

31. Pretel H, Lizarelli RF, Ramalho LT. Effect of low-level laser therapy on bone repair: histological study in rats. *Lasers Surg Med*. 2007;39:788–796.

32. Kazem Shakouri S, Soleimanpour J, Salekzamani Y, Oskuie MR. Effect of low-level laser therapy on the fracture healing process *Lasers Med Sci*. 2010;25:73–77.

33. Kamali F, Bayat M, Torkaman G, Ebrahimi E, Salavati M. The therapeutic effect of low-level laser on repair of osteochondral defects in rabbit knee. *J Photochem Photobiol B*. 2007;88:11–15.

34. Maluf AP, Maluf RP, Brito Cda R, França FM Jr, de Brito RB. Mechanical evaluation of the influence of low-level laser therapy in secondary stability of implants in mice shinbones. *Lasers Med Sci*. 2012;25: 693–998.

35. Dörtbudak O, Haas R, Mailath-Pokorny G. Effect of low-power laser irradiation on bony implant sites, *Clin Oral Implants Res*. 2002;13:288–292.

36. Kim YD, Kim SS, Hwang DS, et al. Effect of low-level laser treatment after installation of dental titanium implant-immunohistochemical study of RANKL, RANK, OPG: an experimental study in rats. *Lasers Surg Med*. 2007;39: 441–450.

37. AboElsaad NS, Soory M, Gadalla LM, et al. Effect of soft laser and bioactive glass on bone regeneration in the treatment of bone defects (an experimental study). *Lasers Med Sci*. 2009;24:527–533.

38. Márquez Martínez ME, Pinheiro AL, Ramalho LM. Effect of IR laser photobiomodulation on the repair of bone defects grafted with organic bovine bone. *Lasers Med Sci*. 2008;23:313–317.

39. Kim YD, Song WW, Kim SS, et al. Expression of receptor activator of nuclear factor -kappaB ligand, receptor activator of nuclear factor-kappaB, and osteoprotegerin, following low-level laser treatment on deproteinized bovine bone graft in rats. *Lasers Med Sci*. 2009;24:577–584.

40. Rochkind S, Kogan G, Luger EG, et al. Molecular structure of the bony tissue after experimental trauma to the mandibular region followed by laser therapy. *Photomed Laser Surg*. 2004;22:249–253.

41. Demidova-Rice TN, Salomatina EV, Yaroslavsky AN, Herman IM, Hamblin MR. Low-level light stimulates excisional wound healing in mice. *Lasers Surg Med*. 2007;39:706–715.

42. Karu T. Photobiology of low power laser effects. *Health Phys*. 1989; 56:691–704.

43. Pinheiro AL, Soares LG, Cangussú MC, Santos NR, Barbosa AF, Silveira Júnior L. Effects of LED phototherapy on bone defects grafted with MTA, bone morphogenetic proteins and guided bone regeneration: a Raman spectroscopic study. *Lasers Med Sci*. 2012;27:903–916.

44. Brawn PR, Kwong-Hing A. Histologic comparison of light emitting diode phototherapy-treated hydroxyapatite-grafted extraction sockets: a same-mouth case study. *Implant Dent*. 2007;16:204–211.

45. Uysal T, Ekizer A, Akcay H, Etoz O, Guray E. Resonance frequency analysis of orthodontic miniscrews subjected to light-emitting diode photobiomodulation therapy. *Eur J Orthod*. 2012;34:44–51.

46. Guzzardella GA, Torricelli P, Nicoli-Aldini N, Giardino R. Osseointegration of endosseous ceramic implants after postoperative low-power laser stimulation: an in vivo comparative study. *Clin Oral Implants Res*. 2003;14: 226–232.

47. Khadra M, Rønold HJ, Lyngstadaas SP, Ellingsen JE, Haanaes HR. Low-level laser therapy stimulates bone-implant interaction: an experimental study in rabbits. *Clin Oral Implants Res*. 2004;15:325–332.